Atmos. Chem. Phys., 14, 4843–4856, 2014
www.atmos-chem-phys.net/14/4843/2014/
doi:10.5194/acp-14-4843-2014

Atmospheric Chemistry and Physics
Open Access

Examining the stratospheric response to the solar cycle in a coupled WACCM simulation with an internally generated QBO

A. C. Kren[1,2], D. R. Marsh[3], A. K. Smith[3], and P. Pilewskie[1,2]

[1]Department of Atmospheric and Oceanic Sciences, University of Colorado at Boulder, Boulder, Colorado, USA
[2]Laboratory for Atmospheric and Space Physics, University of Colorado at Boulder, Boulder, Colorado, USA
[3]National Center for Atmospheric Research, Boulder, Colorado, USA

Correspondence to: A. C. Kren (andrew.kren@colorado.edu)

Received: 8 August 2013 – Published in Atmos. Chem. Phys. Discuss.: 27 September 2013
Revised: 20 March 2014 – Accepted: 6 April 2014 – Published: 16 May 2014

Abstract. The response of the stratosphere to the combined interaction of the quasi-biennial oscillation (QBO) and the solar cycle in ultraviolet (UV) radiation, and the influence of the solar cycle on the QBO, are investigated using the Whole Atmosphere Community Climate Model (WACCM). Transient simulations were performed beginning in 1850 that included fully interactive ocean and chemistry model components, observed greenhouse gas concentrations, volcanic eruptions, and an internally generated QBO. Over the full length of the simulations we do not find a solar cycle modulation of either the QBO period or amplitude. We also do not find a persistent wintertime UV response in polar stratospheric geopotential heights when stratifying by the QBO phase. Over individual ∼40 year periods of the simulation, a statistically significant correlation is sometimes found between the northern polar geopotential heights in February and UV irradiance during the QBO's westerly phase. However, the sign of the correlation varies over the simulation, and is never significant during the QBO's easterly phase. Complementing this is the analysis of four simulations using a QBO prescribed to match observations over the period 1953–2005. Again, no consistent correlation is evident. In contrast, over the same period, meteorological reanalysis shows a strong positive correlation during the QBO westerly phase, although it weakens as the period is extended. The results raise the possibility that the observed polar solar–QBO correlation may have occurred because of the relatively short data record and the presence of additional external forcings rather than a direct solar–QBO interaction.

1 Introduction

Beginning in the 1980s, Labitzke (1987) stratified the mean winter temperatures at 30 hPa over the North Pole by the phase of the QBO (quasi-biennial oscillation) and the January sunspot numbers, a measure of solar cycle variability. Results showed a statistically significant stratospheric difference in the polar stratosphere, such that during QBO west, defined as equatorial westerly winds at 50 hPa, a positive correlation with the solar cycle existed, with warmer polar temperatures and a weaker polar vortex during solar maximum. During the QBO east phase, winter temperatures showed a negative, but insignificant, correlation with the solar cycle. This pointed to a possible influence of the solar cycle on the Holton–Tan relationship (Holton and Tan, 1980), in which the phase of the QBO affects the strength of the stratospheric polar winter vortex. Although the mechanism responsible for QBO influences on the polar vortex is not fully understood (e.g., Garfinkel et al., 2012; Watson et al., 2014), one theory is via the Holton–Tan mechanism. This mechanism states that the waveguide shifts into the Northern Hemisphere (NH) during QBO east, conducive for greater wave dissipation over the northern pole and favoring a polar vortex that is anomalously warm and weak (Holton and Tan, 1980; Thompson et al., 2002; Anstey and Shepherd, 2014). The apparent modulation in the atmospheric response to the QBO over the solar cycle was confirmed by Labitzke and van Loon (1988) over the stratosphere and parts of the troposphere using both temperatures and geopotential heights. The observed relationship was updated in a number of publications during the following decades (e.g., Kodera, 1991;

Labitzke and van Loon, 2000; Gray et al., 2004; Labitzke, 2005; Gray et al., 2006; Camp and Tung, 2007; Lu et al., 2009). Recently, the solar–QBO relationship in the NH polar vortex through 68 years of stratospheric data (1942–2009) was analyzed (Labitzke and Kunze, 2009). Though a relationship is found in the stratosphere at other latitudes and seasons, the strongest correlations are present over the northern polar region in the late-winter (February) period.

There is currently no well-accepted physical mechanism that can explain the apparent stratospheric response due to the 11 year solar cycle and the QBO. If the circulation difference is truly present, it would provide an additional pathway outside of direct surface heating (see for example, Gray et al., 2010) by which solar irradiance variability may influence climate. A number of studies have investigated the relationship using model simulations that incorporated a prescribed, parameterized, or internally generated QBO (e.g., Rind and Balachandran, 1995; Gray et al., 2004; Matthes et al., 2004; McCormack et al., 2007; Schmidt et al., 2010). Although these models have not been able to reproduce all aspects, the studies indicate that there is a circulation response in the polar vortex that depends on both QBO phase and the 11 year solar cycle.

In addition, Salby and Callaghan (2000, 2004, 2006) and Pascoe et al. (2005) have provided some evidence from observations that there exists a decadal variation of both the QBO period and in the duration of the QBO west phase, suggesting that a solar modulation of the QBO may be present. These observations, however, extend over only four solar cycles. A 150 year model simulation study by McCormack et al. (2007) using a parameterized QBO and UV (ultraviolet) variations showed a shortened QBO west period by about 3 months at solar maximum compared to solar minimum. This change in the period was shorter than the observed 3–6 month variation found in Salby and Callaghan (2000), but larger than the ~ 1 month variation found in an earlier model study by McCormack (2003). Fischer and Tung (2008), however, provide results from an equatorial zonal wind data set (1953–2007) showing that the QBO period was anticorrelated with the solar cycle during the first three solar cycles during this period and positively correlated in the latter three cycles. The modulation of the QBO by the solar cycle remains an open question. If there is a response in the QBO to the solar cycle, it is thought to be caused by varying UV radiation, which causes increased heating in the upper stratosphere at solar maximum to produce anomalous easterly momentum to shorten the QBO west period (McCormack, 2003; Pascoe et al., 2005; McCormack et al., 2007). UV radiation exhibits maximum variability of $\sim 3\%$ at 255 nm, the center of the Hartley band (Lean et al., 2005; Gray et al., 2010).

In this study, we analyze the response to both solar and QBO forcing over the whole stratosphere in historical simulations beginning in 1850 in the fully coupled Whole Atmosphere Community Climate Model (WACCM) (Marsh et al., 2013). Section 2 describes the WACCM simulations and methodology. Section 3 discusses the mean solar response in the tropics of WACCM and the influence that the solar cycle may have on the QBO. Section 4 examines the high-latitude response to both solar and QBO forcing and compares it to both the observed record and an ensemble of simulations with a prescribed QBO and observed sea surface temperatures (SSTs). Section 5 summarizes the major conclusions from this study.

2 Methodology

2.1 WACCM

We use WACCM as the atmospheric component of the National Center for Atmospheric Research (NCAR) Community Earth System Model (CESM), denoted CESM1 (WACCM) (Marsh et al., 2013). It extends from the surface to the lower thermosphere (approximately 140 km) with 66 vertical levels of variable vertical resolution of ~ 1.1 km in the troposphere above the boundary layer, 1.1–1.4 km in the lower stratosphere, 1.75 km at the stratopause, and 3.5 km above 65 km; horizontal resolution is 1.9° latitude by 2.5° longitude. Marsh et al. (2013) describe a transient simulation conducted with CESM1 (WACCM) as part of phase 5 of the Coupled Model Intercomparison Project (CMIP5) (Taylor et al., 2012). In these coupled-ocean simulations, CESM1 (WACCM) reproduces many features seen in observations, such as the increase in the observed surface temperature record since 1850, the development of the ozone hole, the frequency and distribution of stratospheric sudden warmings, and the periodicity of the El Niño–Southern Oscillation (ENSO) (Marsh et al., 2013). Some differences are seen compared to observations, for example, a reduced frequency of Atlantic blocking during boreal winter and the minimum in Antarctic sea ice extent. CESM1 (WACCM) represents the 4th major version of the WACCM model and for brevity we refer to it as WACCM4 for the remainder of this paper.

Two WACCM4 historical simulations are analyzed in this paper: the first from the preindustrial period (1850) to the present (2005), denoted as WACCM4a, and the second from 1850 to 1943 (WACCM4b). The experimental setup is described in detail in Marsh et al. (2013), except that these coupled simulations include, for the first time, a QBO internally generated by a parameterization of inertial gravity waves, as described by Xue et al. (2012). Figure 1 shows monthly mean equatorial zonal mean zonal winds in the stratosphere from observations (top) over Singapore (1° N, 104° E) (updated from Naujokat, 1986) and the internally generated QBO (bottom) in WACCM4a. For better visual comparison, we only show the last 10 years of the simulation (1996–2006). As shown by Xue et al. (2012), the internally generated QBO has a latitudinal span of 20° (results not shown), which is in agreement with observations. We note that the timing does not match as would be expected since the QBO is internally generated; the period, however, is close to observed (discussed in Sect. 3) at around 28 months. The peak amplitude of the QBO is strongest during the east phase at $\sim 30\,\mathrm{m\,s^{-1}}$, while westerlies are weaker, between ~ 15 and $20\,\mathrm{m\,s^{-1}}$, also consistent with the observed QBO. Two potential shortcomings are noted of the internally generated QBO in both WACCM4 simulations, and are evident in Fig. 1: QBO westerlies are longer lasting than easterlies in the mid- to upper stratosphere, a result contrary to that in observations (Baldwin et al., 2001); the QBO does not descend to 100 hPa and, in particular, the west phase does not reach 50 hPa.

The WACCM4 simulations produce differences in the high latitudes as a function of the QBO (not shown) that are similar in magnitude and timing to the observed Holton–Tan variations (e.g., Pascoe et al., 2005; Lu et al., 2008; Naoe and Shibata, 2010; Anstey and Shepherd, 2014). A statistically significant (95 % using two-sided t test) response is seen in the high latitudes in November between 1 and 70 hPa with a magnitude change of ~ 4 K in WACCM4a. Differences are also seen from December to March, which appear to descend with time, but are not statistically significant. Corresponding zonal mean zonal wind changes are also present on the order of $\sim 6\,\mathrm{m\,s^{-1}}$ in November. In WACCM4b, the signal is statistically significant at 95 % throughout the winter season and descends into the lower stratosphere from November to February (between 1 and 100 hPa) with zonal winds changes of 8–12 $\mathrm{m\,s^{-1}}$. Thus, WACCM4 reasonably shows a weaker polar vortex in the QBO east phase, with magnitude changes comparable to reanalysis data of 7–10 $\mathrm{m\,s^{-1}}$ and 3–4 K (e.g., Lu et al., 2008; Naoe and Shibata, 2010).

As in the WACCM4 CMIP5 simulations, the simulations presented here include changing greenhouse gases, specified volcanic activity, interactive ocean, chemistry, and sea ice. Solar spectral irradiance (SSI) input to the model is based on observations and is taken from the Navy Research Laboratory Solar Spectral Irradiance (NRLSSI) model (Lean et al., 1997, 2005; Lean, 2000). The NRLSSI values are scaled by 0.9965 to agree with the new estimates of total solar irradiance (TSI) from the total irradiance monitor on the NASA Earth Observing System Solar Radiation and Climate Experiment satellite (Rottman, 2005). This newest TSI measurement shows an irradiance of $1360.8 \pm 0.5\,\mathrm{Wm^{-2}}$ over the recent solar minimum in 2008, lower than previous estimates of TSI (Kopp and Lean, 2011). SSI is constructed using a combination of satellite measurements from the SOLar STellar Irradiance Comparison Experiment (SOLSTICE) and SOLar SPECtrum instruments (SOLSPEC; Rottman et al., 2004; Thuillier et al., 2009), multiple regression, and parameterizations of sunspots and faculae influences (sunspot darkening and facular brightening) based on their location and size across the solar disk (Lean, 2000; Lean et al., 2005). Although uncertainty exists in reconstructing SSI before the space age, several proxies are used, including the geomagnetic aa index (Lockwood and Stamper, 1999), cosmogenic isotopes in both tree rings and ice cores (Bard et al., 2000), observed variations in Sun-like stars (Baliunas and Jastrow, 1990), and flux-transport models to understand the magnetic flux across the disk since 1713 (Lean et al., 2005). The NRLSSI model agrees well with observations when integrated over all wavelengths. When compared to other SSI models and observations, differences of up to a factor of 3 are present at UV wavelengths (Ermolli et al., 2013). Although the NRLSSI model represents the lower limit of SSI variability, uncertainty in both observations and models make it difficult to assess the solar cycle variations.

Also included in the WACCM4 simulations are auroral variations driven by the planetary geomagnetic index (Kp), as discussed in Marsh et al. (2007). Higher energy particle precipitation that penetrates into the middle to lower atmosphere is not simulated. The absence of these higher energy particles possibly underestimates the energetic particle impacts over the solar cycle. If these particles play a role in the dynamical response of the stratosphere to the solar cycle, their impact will not be seen in the WACCM4 simulations.

We complement our WACCM4 simulations with an ensemble of four WACCM3.5 simulations performed for the Chemistry-Climate Model Validation (CCMVal-2) project (SPARC CCMVal, 2010). These transient simulations were forced with the same time-varying SSI as in the WACCM4 runs and also include volcanic eruptions (Tilmes et al., 2009), greenhouse gases, and evolving ozone-depleting substances. Two differences in the CCMVal-2 runs compared with our two WACCM4 runs are that SSTs are specified from observations and the QBO was included by relaxing equatorial stratospheric winds to observations (Matthes et al., 2010). WACCM3.5 climatological global mean temperature and trends in the stratosphere are in good agreement with the observational record (SPARC CCMVal, 2010). Chiodo et al. (2012) found that the ensemble mean showed a realistic representation of the solar signal in the tropical stratosphere. In ozone and temperature, a double peak structure was present over the lower and upper stratosphere. At the high latitudes, the ensemble mean showed a strengthening of the polar vortex in NH winter during solar maximum, along with the downward propagation of zonal wind anomalies through changes in planetary wave propagation and the Brewer–Dobson circulation, consistent with the model from Kodera and Kuroda (2002). One exception is that the ensemble members differed in regards to both the magnitude and timing of the zonal wind response.

2.2 Observational data sets

Both our WACCM4 simulations and the CCMVal-2 ensemble run are compared to the observational record (1953–2012). We use geopotential height data from NCEP-NCAR reanalysis from 1953 to 2012 (Kalnay et al., 1996). In addition, we use the observed monthly mean equatorial zonal wind data set at 50 hPa, comprised of radiosonde data from Canton Island (3° S, 172° W) from January 1953 to August

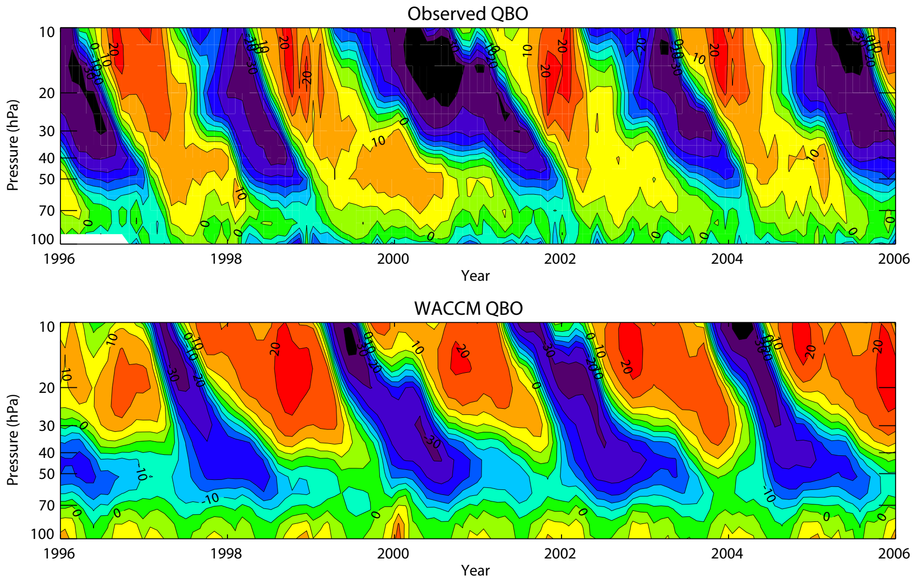

Fig. 1. Contour plot of the monthly mean equatorial zonal winds between 10 and 100 hPa from both observations (top) over Singapore (1° N, 104° E) and the internally generated QBO in WACCM4a (bottom). Time period is from 1996 to 2006. Amplitude is in meters per second with contour interval of 5 m s^{-1}. Blue shading indicates QBO easterlies and red/orange denotes QBO westerlies. Singapore observations are available at http://www.geo.fu-berlin.de/en/met/ag/strat/produkte/qbo/index.html.

1967, Gan Island, Maldives, (1° S, 73° E) from September 1967 to December 1975, and Singapore (1° N, 104° E) since January 1976 (updated from Naujokat, 1986). This data set is available at http://www.geo.fu-berlin.de/en/met/ag/strat/produkte/qbo/. We use the observed radiosonde winds as reanalysis data show a much lower QBO magnitude compared to radiosonde observations. This reduced magnitude is likely due to the lack of rawinsonde observations, as pointed out by Kistler et al. (2001).

2.3 Analysis methods

The majority of this paper uses composite analysis based on phases of the solar cycle and QBO. In this section, we present definitions of solar maximum and minimum and the QBO east and west phases. We also discuss our composite analysis and Monte Carlo sampling using the two WACCM4 simulations.

For examining the solar cycle response in WACCM4, we group years into solar maximum and minimum using the NRLSSI 255 nm spectral irradiance because it is at the center of the Hartley band (Marsh et al., 2007), where absorption of UV radiation by ozone is maximum (Gray et al., 2010), and therefore is appropriate for detecting a stratospheric solar cycle temperature response from ozone heating. In addition, the 255 nm spectral irradiance is highly correlated (0.96 over the full simulation of WACCM4a) to the solar 10.7 cm solar radio flux, a frequently used proxy for solar activity. In stratifying solar maximum and minimum years, we focus on the peaks and troughs in the solar cycle. We first calculate a 3 year running mean of the annually averaged 225 nm spectral irradiance. From this time series, we select the 3 years that make up a local maximum and minimum for each cycle in the running mean. Figure 2 shows the annually averaged 255 nm spectral irradiance (in mW m^{-2} nm^{-1}) from 1850 to 2005 and the years identified occurring at solar maximum and minimum. There are a total of 45 solar maximum years and 42 solar minimum years.

Next, we define the QBO east and west phases in both our model simulations and observations. As discussed in Sect. 2.1, the internally generated QBO in WACCM4 does not penetrate to 50 hPa, most evident during the west phase. As a result, similar to several studies that include a simulated QBO with insufficient descent (e.g., Giorgetta et al., 2002; Palmer and Gray, 2005; Giorgetta et al., 2006; Schmidt et al., 2010), we define the period and phase of the QBO in our WACCM4 simulations from the model winds at 30 hPa. Due to the asymmetry of the QBO, we follow Chiodo et al. (2012) and define westerlies when the monthly mean equatorial wind at 30 hPa is greater than 5 m s^{-1} and easterlies when below -10 m s^{-1}. In both our CCMVal-2 and radiosonde observations, we define the period and phase of the QBO at 50 hPa. QBO east and west are defined as in our WACCM4 runs. Because the CCMVal-2 equatorial zonal mean zonal winds were relaxed to match the radiosonde observations defined in Sect. 2.2, we use the radiosonde wind data set described in Sect. 2.2 to define the QBO in the CCMVal-2 simulations.

When performing composite analysis to examine the solar cycle and QBO response of the stratosphere, we stratify the

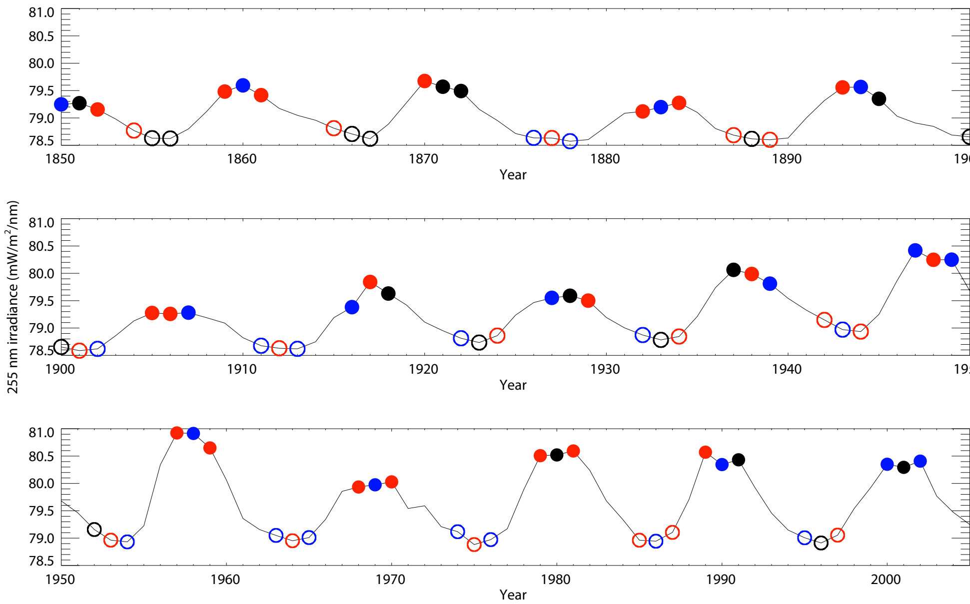

Fig. 2. The annually averaged 255 nm spectral irradiance (mW m^{-2} nm^{-1}) from Lean et al. (2005) for the periods 1850-1900 (top), 1900–1950 (middle), and 1950–2005 (bottom). Filled circles represent solar maximum years and open circles represent solar minimum years, determined using a 3 year running mean of the annual 255 nm spectral irradiance and choosing the 3 years that make up a local maximum and minimum for each cycle. Blue colored circles (open and filled) denote years in WACCM4a when the QBO in February (during solar maximum or minimum) was east and red circles when the QBO in February was west. Black open and filled circles denote years when the QBO was neither east nor west using the criteria defined in Sect. 2.3.

data according to the phase of the solar cycle and QBO as described above. The analysis fields include monthly mean wind and geopotential height data from both our model simulations, reanalysis data, and observations. The statistical significance in the solar–QBO response is determined using a two-sided significance test. Because the WACCM4 and CCMVal-2 simulations include increasing greenhouse gases into the 21st century, the geopotential height data is detrended to remove any linear increase due to anthropogenic forcing.

We also investigate the mean response of the polar solar–QBO response. To do this, we perform Monte Carlo sampling using both WACCM4 simulations. To perform the random sampling, we focus on the winter season (December, January, February, and March) and combine the two WACCM4 runs to create a total of 249 years of winter data. For each winter month, we group the years into east and west. Then for each east and west group, we randomly select 16 east and 33 west winters to match with the number of east and west years in the 1953–2012 observational record. We then compute the correlation between the 30 hPa geopotential heights at the North Pole and the 255 nm spectral irradiance. This is performed a million times and repeated for each winter month. The result is a normalized histogram of the correlation (R) for east and west phases for each month.

3 Solar cycle response in the tropics

We first examine the solar cycle response in WACCM4a by computing the difference in annual average detrended temperatures (in K) between solar cycle maximum and minimum (as identified in Fig. 2) in the stratosphere. The response is averaged over the equatorial region from 25° S to 25° N. The result is shown in Fig. 3. The response in stratospheric temperature shows the double-peak structure seen in observations and past model simulations. In the tropical lower stratosphere, there is a temperature change of ∼ 0.3 K between solar minimum and maximum near 50 hPa. This lower stratospheric change below 50 hPa, however, is not significant, as evidenced by the large uncertainty of 1.5–2 K. Another change of ∼ 0.5 K is present in the upper stratosphere just below 1 hPa. These results are in agreement with results from a suite of several coupled chemistry climate models by Austin et al. (2008), showing that the model mean temperature change is ∼ 0.5 K in the upper stratosphere. The temperature changes are consistent with observations in the lower and upper stratosphere from ERA-40 (European Centre for Medium-Range Weather Forecasts (ECMWF) 40 year Re-Analysis) data (Chiodo et al., 2012), but the solar cycle response in WACCM4 (∼ 0.5 K) is lower than the ∼ 1 K change in observations. The combined solar cycle and QBO response in the atmosphere is examined in Sect. 4.

We next examine if the amplitude or phase of the QBO in WACCM4a is modulated by the solar cycle by segregating

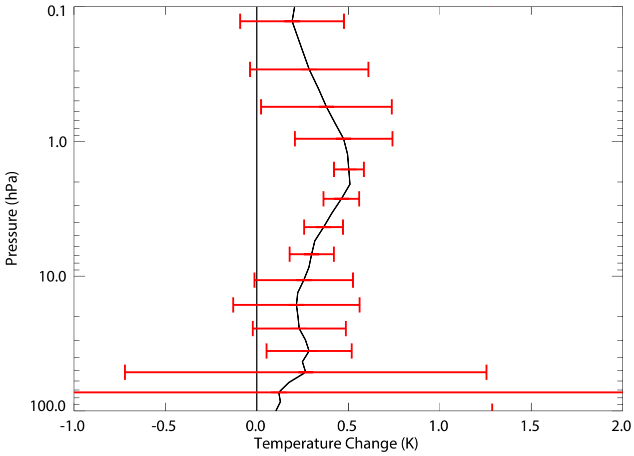

Fig. 3. Annual average temperature change (K) over the solar cycle (solar maximum minus solar minimum) between 100 and 0.1 hPa in WACCM4a, averaged over the latitude band 25° S–25° N. Red error bars denote the 2σ uncertainty. For emphasis, we show the zero temperature change by the vertical black solid line.

Table 1. The mean and standard deviation of the QBO amplitude and duration for both east and west phases in WACCM4a as a function of solar maximum (Max) and solar minimum (Min) years.

	Amplitude ($\mathrm{m\,s^{-1}}$)		Duration (months.)	
	Max	Min	Max	Min
East	27.1 ± 2.8	26.9 ± 4.9	10.5 ± 3.0	10.5 ± 2.9
West	17.5 ± 2.0	16.4 ± 2.2	14.7 ± 2.2	14.6 ± 2.9

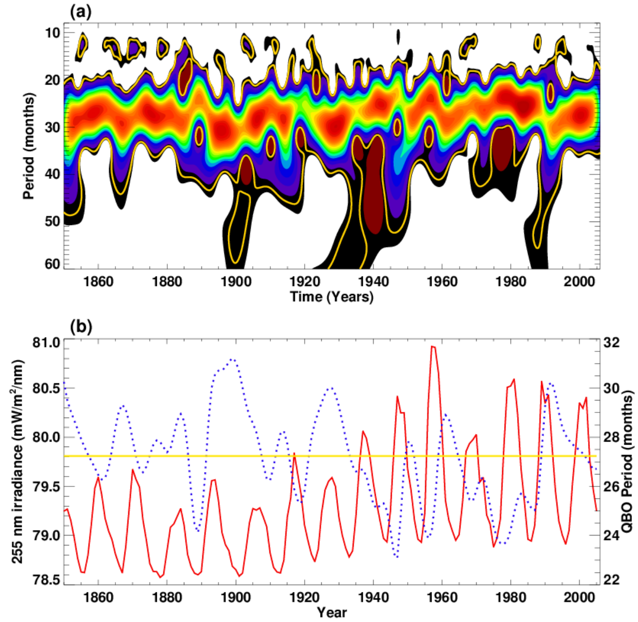

Fig. 4. (a) Wavelet power spectrum of the QBO at 30 hPa, showing the dominant period of the QBO and its variability with time through the entire WACCM4a simulation. Color shading denotes the power. Bottom x axis denotes the time (years) and left y axis corresponds to the period (in months) of the QBO. Yellow solid contours enclose regions greater than 95 % confidence. Wavelet software provided by C. Torrence and G. Compo, is available at http://paos.colorado.edu/research/wavelets/. More information on wavelet analysis is provided in Torrence and Compo (1998). **(b)** The annually averaged 255 nm spectral irradiance (red solid line) from Lean et al. (2005), along with the variation in the QBO duration in months (blue dashed line) in WACCM4a. The variation in the QBO period is determined from the wavelet power spectrum, as described in Sect. 3. Yellow line denotes the average QBO period over the entire model simulation (27.2 months).

the solar maximum and minimum years identified in Fig. 2 by the phase of the QBO. First, we detrend the zonal mean zonal wind. We determine the length (in months) of each QBO east and west period by the zero wind crossing. Periods where the length of QBO east and west is shorter than 3 months are excluded. The peak amplitude ($\mathrm{m\,s^{-1}}$) is defined as the maximum zonal mean zonal wind in each QBO east and west period. We then segregate the data into years of solar maximum and minimum and compute the mean and standard deviation of the length (duration) and amplitude for east and west QBO. Table 1 lists the mean and standard deviation of the peak QBO amplitudes and the duration of QBO phases grouped by years of solar maximum and minimum. The average peak QBO winds are $\sim 27\,\mathrm{m\,s^{-1}}$ in the east phase and $\sim 17\,\mathrm{m\,s^{-1}}$ in the west phase. The peak winds and duration of east and west phases exhibit no statistically significant difference between minima and maxima in the solar cycle.

In addition, to further examine the possible modulation of the QBO period by the solar cycle, we compute a Morlet wavelet power spectrum (Torrence and Compo, 1998) of the equatorial monthly zonal mean zonal winds at 30 hPa in WACCM4a (shown in Fig. 4a). Figure 4a clearly shows that the variation in the spectral power of the QBO is present at timescales between 23 and 38 months. For each month, we can determine the QBO period as the period for which the power spectrum shown in Fig. 4a reaches its maximum. Averaging those monthly periods over a year gives the average QBO period for the year. Figure 4b shows the time series of the QBO period in WACCM4a along with the yearly 255 nm spectral irradiance. Averaged over the entire model simulation, the average QBO period is 27.2 months, again consistent with the observed period (Baldwin et al., 2001). The correlation between the yearly 255 nm spectral irradiance time series and QBO period is −0.24. When dividing the period up into three segments, the correlation is positive (0.12) from 1850 to 1899, switches sign (−0.41) from 1900 to 1949, and is −0.03 from 1950 to 2005. The varying sign of the correlations indicate that the QBO period is not modulated directly by the solar cycle. There may be other external forcings or internal variability at play impacting the QBO period.

4 High latitude stratospheric response to solar and QBO forcing

4.1 High latitude response in February

In Sect. 2.1, we described the high latitude response to the QBO winds that was similar in magnitude and timing to the observed Holton–Tan variations. In this section, we present the high latitude stratospheric response to both the solar cycle and QBO and compare to past observational and modeling studies. We investigate the high latitude response in late winter. The largest change in the polar vortex in the observed record to the combined solar–QBO interaction was found in February (Labitzke and Kunze, 2009). For comparison to the results of Labitzke and Kunze (2009), we plot the monthly mean geopotential heights at 30 hPa at 90° N in February as a function of the solar cycle and separated by the QBO phase. Figure 5 shows the geopotential heights for both QBO east and west versus the 255 nm spectral irradiance, along with linear regression fits. Figure 5 shows that there is no strong correlation between the solar cycle and geopotential heights at the northern pole over either QBO phase, as evidenced by the weak correlations.

Table 2 shows the correlations for ∼ 40 year periods starting in 1850 between the 30 hPa geopotential heights at 90° N in February and the 255 nm spectral irradiance for QBO east and west in both WACCM4 simulations. Using the 90 % level as a threshold for significance, the polar solar–QBO correlation is seen only in WACCM4a during the west phase in the period 1891–1931 with a correlation of 0.43. The east phase periods in WACCM4a and both east and west phases in WACCM4b do not show a statistically significant response. This response during the west phase seen in WACCM4a has a different sign when evaluated over the period 1973–2005, with a negative correlation of −0.47 (91 % level). These results show that WACCM4a can reproduce the solar–QBO correlation over short 40 year periods and, at times, agrees with past observational and modeling studies (e.g., Rind and Balachandran, 1995; Matthes et al., 2004; Labitzke and Kunze, 2009). But the response is not consistent among the two WACCM4 simulations and does not persist over the full simulation periods.

To complement these WACCM4 results we show results from the ensemble of four WACCM3.5 CCMVal-2 simulations that were run from 1953 to 2005 and are also listed in Table 2. Again, using the 90 % level as a threshold for significance, none of the CCMVal-2 simulations show a statistically significant polar solar–QBO correlation for both east and west QBO phases. All of the CCMVal-2 runs show a negative correlation in the east phase of the QBO, but the correlations are not significant. In the west phase, three of the CCMVal-2 runs show positive correlations, but again are not statistically significant. This conclusion was also found by Chiodo et al. (2012), who analyzed the zonal wind response in the same CCMVal-2 ensemble; they found that the apparent polar vortex response was not reproduced in all ensemble members.

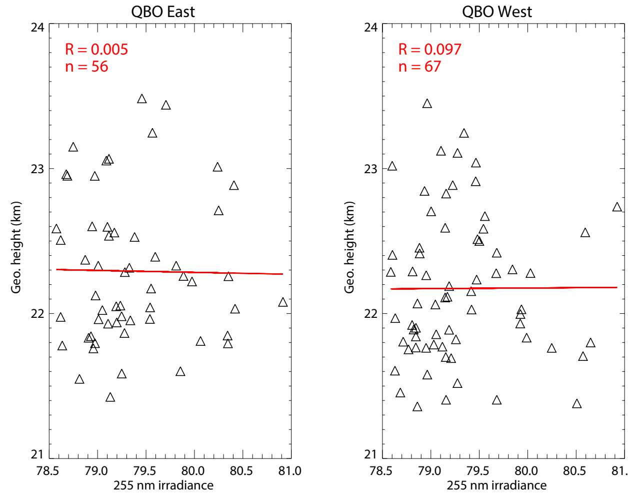

Fig. 5. Scatter diagram of the monthly mean 30 hPa geopotential heights (km) at 90° N in February plotted against the 255 nm spectral irradiance during QBO east (left) and QBO west (right). Triangles represent the individual years over the model simulation (1850–2005) in WACCM4a; n denotes the number of years in QBO east and west, and *R* is correlation coefficient between the 255 nm spectral irradiance (m $\mathrm{W m^{-2}\,nm^{-1}}$) and geopotential heights.

To compare our results from both WACCM4 and CCMVal-2 to the observed record, we also include in Table 2 the correlations using both NCEP-NCAR reanalysis data of monthly mean geopotential height and the observed equatorial stratospheric winds (as discussed in Sect. 2.2). Two periods are analyzed: 1953–2005 and 1953–2012. Over both periods, observations show no statistically significant response during the east phase of the QBO, consistent with our WACCM4 and CCMVal-2 runs. During the west phase of the QBO, a statistically significant (99 %) response is found with a correlation of 0.61 from 1953 to 2005, consistent with Labitzke and Kunze (2009). A significant correlation was also found in WACCM4a from 1891 to1931 but not in WACCM4b. The correlation in the observed record for QBO west decreases to 0.36 (96 % significant) in the longer period from 1953 to 2012, and suggests than an extended period may lead to a weaker response, consistent with the results in WACCM4a and in Fig. 5. Although not shown, we also compute the correlation between the 30 hPa geopotential heights at 90° N in February and the 255 nm spectral irradiance for QBO east and west when the observed QBO is defined at 30 hPa, as in our WACCM4 simulations. The response in the west phase shows the same sign as that when the QBO is defined at 50 hPa with a correlation of 0.32 (1953–2012), although the significance lowers to 86 %. These observational results indicate that the 30 hPa level used to define the QBO in WACCM4 will not significantly alter the results.

Table 2. Variation in the Spearman rank correlation between the 30 hPa geopotential heights in February at 90° N and the 255 nm spectral irradiance for the QBO east and west phases. Results are for this study (WACCM4a, WACCM4b), four CCMVal-2 simulations, and NCEP-NCAR Reanalysis with stratospheric wind observations (1953–2005 and 1953–2013) from Canton Island (3° S, 172° W), Gan Island/Maldives (1° S, 73° E), and Singapore (1° N, 104° E); n denotes the number of years in each respective phase. Values in brackets indicate the two-sided significance level of the correlations. Bold denotes the correlations with significance values above 90 %.

Model/ Obs.	Period	QBO East	QBO West	n (East)	n (West)
WACCM4a	1850–1890	−0.04 [0.89]	0.22 [0.36]	11	18
WACCM4b	1850–1890	−0.17 [0.58]	−0.13 [0.57]	11	18
WACCM4a	1891–1931	0.06 [0.83]	**0.43 [0.08]**	16	18
WACCM4b	1891–1931	−0.24 [0.34]	0.04 [0.87]	16	18
WACCM4a	1932–1972	−0.07 [0.77]	−0.04 [0.87]	16	17
WACCM4a	1973–2005	0.00 [0.98]	**−0.47 [0.09]**	13	14
CCMVal-2a	1953–2005	−0.08 [0.77]	0.11 [0.59]	14	28
CCMVal-2b	1953–2005	−0.03 [0.89]	−0.29 [0.12]	14	28
CCMVal-2c	1953–2005	−0.02 [0.93]	0.08 [0.67]	14	28
CCMVal-2d	1953–2005	−0.06 [0.82]	0.04 [0.84]	14	28
Reanalysis	1953–2005	−0.09 [0.73]	**0.61 [0.001]**	14	28
Reanalysis	1953–2012	−0.18 [0.47]	**0.36 [0.04]**	16	33

4.2 Monte Carlo sampling

The previous section has shown that the correlations between polar geopotential heights and the solar cycle for each phase of the QBO varies considerably depending on the period analyzed. To examine the time-mean response we randomly sample winters from both WACCM4 simulations (a total of 249 years). We focus on the winter season (December, January, February, and March), and, for each winter month, group the years into QBO east and QBO west. From each east and west group, we randomly select 16 east and 33 west winters to match with the number of east and west years in the 1953–2012 observational record. We then compute the correlation between the 30 hPa geopotential heights at the North Pole and the 255 nm spectral irradiance. This is performed a million times and repeated for each winter month. Figure 6 shows the normalized histogram of R between the 255 nm irradiance and the geopotential heights at the northern pole for east and west phases in each month. During the east phase, the curve is centered near zero in January and March, implying an equal chance of getting either a positive or negative correlation; the mean correlation is negative in December and February, with the highest magnitude in February at −0.08. For the QBO west phase, a positive mean correlation is found only in December with a mean R of ~ 0.13; the correlation is negative from January to March. This would imply agreement with the sign of the correlation found by Labitzke and Kunze (2009) in early winter, followed by a reversal starting in January that exhibits the same correlation as during QBO east. However, the correlations in early winter are much smaller than those found in Labitzke and Kunze (2009). The statistics shown in Fig. 6 can be used to determine the probability of getting the result found in the observational record from 1953 to 2012, that is, a correlation in the east phase that is less than −0.18 and a correlation in the west phase that is greater than 0.36. The highest probability in QBO east was found in February with 34 %; the highest probability in QBO west was in December with 6 %. These results state that the solar–QBO correlation is not reproduced in the long-term time mean.

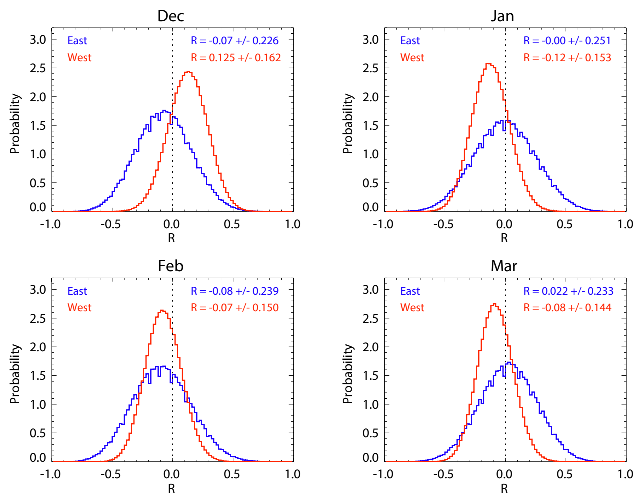

Fig. 6. Monte Carlo sampling plots showing the normalized probability of R between the 30 hPa geopotential heights at the North Pole and the 255 nm spectral irradiance for December, January, February, and March as a function of QBO east (blue) and west (red) from the combined WACCM4 simulations. Dotted line represents zero correlation and is shown to emphasize the mean change in R. The mean and standard deviation of R for each QBO phase is listed at the top right of each month. A bin width of 0.02 was used to create the histogram.

4.3 Seasonal QBO signal over the whole stratosphere

In the previous section, we examined the correlation between the geopotential heights at 30 hPa and at 90° N and the 255 nm spectral irradiance as a function of the QBO east and west phases for only February. In this section, we investigate the correlation in the geopotential heights (at all pressure levels) at 90° N with the 255 nm spectral irradiance for QBO phases for each month of the year to see if a response was present at other times of the year. Figure 7 shows the correlation as a function of pressure level and month between 1000 and 0.01 hPa for QBO east and west in the 1850–2005 WACCM4a simulation. While there are statistically significant positive and negative correlations during both phases, because these correlations are of the same sign it points to an interaction regardless of QBO phase. Furthermore, these significant correlations occur primarily in late summer and autumn; there is no significant response in late winter over the depth of the stratosphere.

We also examine the circulation response by computing the difference in the zonal mean geopotential heights, temperature, and zonal mean zonal wind between solar maximum and minimum years for the QBO east and west phases over the whole stratosphere (results not shown) for both WACCM4 simulations. On the annual average, we see statistically significant differences in the heights and temperature over the thermosphere independent of QBO phase that are likely due to extreme UV variations impacting the density. When stratifying to both the QBO phase and solar cycle, we find the greatest signal in the monthly average polar vortex differences from December to February. During QBO east, both WACCM4 cases show comparable magnitude changes of ~ 8–$12\,\mathrm{m\,s^{-1}}$ over the northern polar region between solar maximum and minimum. However, the two cases differ in regards to the actual atmospheric response. In WACCM4a, the response is opposite of what was found by Labitzke and Kunze (2009). That is, the circulation response shows a weaker polar vortex during solar maximum. In WACCM4b, the response shows a stronger polar vortex during solar maximum only in February. The circulation responses in both WACCM4 cases are not statistically significant. In the QBO west phase, a statistically significant circulation response (90 %) in agreement with Labitzke and Kunze (2009) is found in February in WACCM4b with zonal wind changes on the order of $\sim 12\,\mathrm{m\,s^{-1}}$. The signal descends into the lower stratosphere in March but is not statistically significant. The response is the opposite in WACCM4a, showing a stronger polar vortex in solar maximum in December and January of 8–$10\,\mathrm{m\,s^{-1}}$ (90 % significance in December). To summarize, while both WACCM4 cases show some indication of a polar vortex change with respect to composites of solar and QBO phase, the two cases fail to show both a consistent pattern and a seasonal progression through the winter season, contrary to past modeling studies using a prescribed or internally generated QBO (e.g., Balachandran and Rind, 1995; Rind and Balachandran, 1995; Matthes et al., 2004, 2010, 2013; Palmer and Gray, 2005; Schmidt et al., 2010); this may indicate that the apparent circulation changes discussed above may be related more to internal variability in the polar winter vortex in WACCM than any solar–QBO interaction.

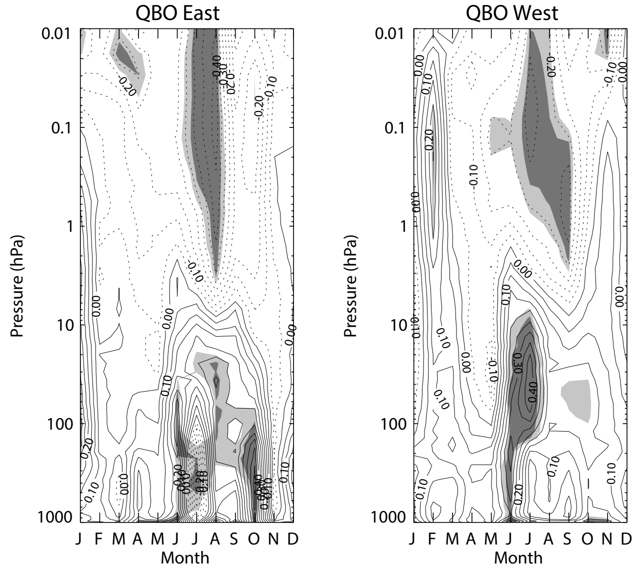

Fig. 7. Contour plot of the Spearman rank correlation between the monthly averaged geopotential heights at 90° N, as a function of pressure level and month, and the 255 nm spectral irradiance for both the QBO east (left) and west (right) phases in WACCM4a. Light and dark shading indicates the significance of the correlations (90 % and 95 %) using a two-sided significance test. Contour interval 0.05. Negative values are dashed.

5 Summary and discussion

Results were presented from two WACCM4 simulations including fully interactive ocean, sea ice, and chemistry components, varying solar spectral irradiance, volcanic forcing, and an internally generated QBO. In an expansion beyond the capabilities of past modeling studies investigating the solar–QBO interaction at high latitudes, these model simulations include a time-varying solar cycle, interactive ocean, and durations of 156 and 93 years, longer than what was examined in prior studies. This facilitated a comprehensive analysis on the solar cycle response. Over the tropical stratosphere, a solar cycle change in temperature is evident in WACCM4a, with an increase of ~ 0.5 K in the upper stratosphere and ~ 0.3 K in the lower stratosphere during solar maximum conditions; however, the lower stratospheric change is not significant. While the temperature changes are at the lower end compared with ERA-40 data (Chiodo et al., 2012), the pattern is consistent with observations and past modeling studies.

We also examined the interaction of the solar cycle on the QBO period and amplitude in WACCM4a. Segregated into solar maximum and minimum years, the lengths and amplitudes of QBO east and west phases do not show a statistically significant difference, consistent with the findings of Schmidt et al. (2010), who used an internally generated QBO in the HAMMONIA (Hamburg Model of the Neutral and Ionized Atmosphere) model. Using a Morlet wavelet power spectrum to calculate the variation in the QBO period as a function of year, the correlation with the solar cycle was −0.24 over 156 years in WACCM4a. This correlation changes sign over ∼ 40 year periods, indicating the change in the QBO period is not directly forced by the solar cycle. This result is in agreement with Fischer and Tung (2008), who analyzed an equatorial zonal wind data set (1953–2007) and found that while the QBO period was anticorrelated with the solar cycle during the first three solar cycles, it became positively correlated in the latter three cycles. There is one caveat regarding our internally generated QBO: since the internally generated QBO in the WACCM4 simulations is forced primarily by a parameterization of inertial gravity waves (Xue et al., 2012), the source of the waves is largely deterministic. However, once the waves propagate into the stratosphere, any potential modulation of these waves (such as from changes in stratospheric ozone and heating), and thereby the QBO, are well represented in WACCM. Given this caveat, our study does not find a modulation of the QBO by the solar cycle.

A specific goal of the analysis was to investigate the well-documented observed correlation of NH winter polar fields in the stratosphere with the solar cycle when the months are stratified by the phase of the QBO (Labitzke and Kunze, 2009). If the model simulated the observed pattern, we could use the model to probe the dynamical or radiative mechanisms that lead to the observed correlations. The examination of the high latitude response over selected ∼ 40 year periods in WACCM4a shows that during the QBO west phase, WACCM4a can successfully reproduce the observed polar solar–QBO correlation over short periods, similar to the observational record. This correlation, however, changes sign through the simulation and is not found in either 40 year period of WACCM4b. When examining the time-mean response over 249 simulation years, results of the stratospheric response to the solar cycle and QBO phase do not show a statistically significant correlation at the northern pole in either WACCM4 simulations, in late winter over the depth of the stratosphere. A significant correlation between the solar cycle and geopotential heights was found in late summer and autumn in WACCM4a, but it exhibited the same sign for both QBO phases, suggesting little in the way of a QBO interaction. During short 40 year periods, other external forcings such as volcanic aerosols, ENSO, and internal variability may dominate over the solar cycle signal and interact with or reinforce each other to produce an apparent solar–QBO response. If the forcing processes are not correlated, then the atmospheric responses to each will become easier to separate when the time series is longer. Over the full simulation of 156 years in WACCM4a, a potential QBO-solar cycle signal should therefore be more apparent, which is not found in our results.

To further examine the time-mean response of both solar cycle and QBO influences on the high latitudes, we performed Monte Carlo sampling by combining both WACCM4a and WACCM4b simulations. Results showed a low probability of achieving the response seen by Labitzke and Kunze (2009). The implication of the reversal in the solar–QBO correlation seen in the QBO west phase in Fig. 6 is unclear. The reversal could be attributable to internal variability of the polar vortex in WACCM4 through the winter season, irrespective of a combined solar–QBO interaction.

Data from several additional WACCM simulations were used to check the results. Analysis of an ensemble of four WACCM3.5 CCMVal-2 simulations using a prescribed QBO also failed to reveal a statistically significant correlation of the NH polar stratosphere to the combined effects of solar cycle and QBO. These runs have a QBO specified from observations, thereby alleviating concerns that the structure of the internally generated QBO in WACCM was not capable of capturing the observed relationship. One of the shortcomings of the WACCM4 simulations with self-generated QBO are the lack of descent of the QBO to 100 hPa, in particular during the QBO west phase, which stops above 50 hPa. It is possible that this lack of descent may impact the high latitude response through a possible lack of interaction of the QBO with planetary-scale waves, leading to a damped response over the polar winter stratosphere. We note, however, that the ensemble of WACCM3.5 simulations using a prescribed QBO also did not show a robust high latitude response from solar and QBO forcing. Thus the shortcoming of the vertical extent of the modeled QBO is not the reason that the model was unable to reproduce the observed correlation.

In both the model and in the atmosphere, the QBO period varies from cycle to cycle but is in the range of 24–30 months. However, when looking at a particular calendar month, the effective period has additional components, as pointed out by Salby and Shea (1991). The longest timescale that emerges from the beating between a 12 month annual cycle and a regular 28 month QBO is 7 years. For a 27 month QBO the timescale is 9 years. This timescale will contribute to time series analysis of single seasons or calendar months, including analysis stratified by the phase of the QBO. It will not affect the Monte Carlo analysis performed in this study. This factor may contribute to the lower probabilities found from the Monte Carlo analysis.

Another issue for the analysis of observations is the presence of additional external forcings. The primary candidate is the irregular occurrence of volcanic eruptions that are strong enough to perturb the radiative balance of the stratosphere. The 1982 eruption of El Chichón and the 1991 eruption of Mt Pinatubo both caused substantial perturbations to the global stratosphere that persisted for several years. Both occurred during periods of high solar activity and have been suspected of contaminating the analysis of the response to solar variability (e.g., Lee and Smith, 2003; Chiodo et al., 2013). The WACCM4 simulations presented here include a much longer span of years, so the percentage of periods that have high solar activity and also have aerosol distributions characteristic of major volcanic eruptions is much smaller. This likely reduces the impact of this potential complication.

An analysis including additional years indicates that the impact of the length of the analysis period is evident from the observational record. The solar–QBO correlation in the west phase decreased when the period of record was extended to 2012 compared with 1953–2005, suggesting that an extended period of record may lead to a weaker response. This is consistent with our model results that reproduce the observed solar–QBO correlation over short periods but not in the long-term time mean. Our use of the 30 hPa winds to define the phase of the QBO did not alter the solar–QBO correlations in WACCM4. This has some support since correlations with high latitude observations also have a similar response when 30 hPa, instead of 50 hPa, is used to define the QBO phase in observations.

Recent observations (i.e., Lu et al., 2009) and model simulations (Schmidt et al., 2010; Matthes et al., 2013) continue to show a circulation response over the high latitudes that depends on both QBO phase and solar cycle forcing. Schmidt et al. (2010) performed two perpetual solar maximum and minimum simulations using an internally generated QBO, each with 42 years in length; they found a significant change in March with a more disturbed polar vortex during QBO west in solar maximum. Matthes et al. (2013) performed an improved simulation over Matthes et al. (2010) by changing from strictly perpetual solar maximum/solar minimum runs to adding a varying solar cycle with 110 years simulated using a prescribed QBO. The result was a statistically significant circulation difference when stratified according to QBO phase and solar cycle. From the results using our WACCM4a simulation, we find agreement with these current and past modeling studies (i.e., Rind and Balachandran, 1995) in that the observed polar solar–QBO correlation in late winter is sometimes present, as shown in Table 2. Over a short record of ~ 40 years, our results are consistent with those of Schmidt et al. (2010), who used a model that also included an internally generated QBO. The caveat is that when the period is extended beyond the length of the observational record, the correlation switches sign in WACCM4a and thus the solar–QBO dependency is not robust throughout the full simulation.

Our results are the first to incorporate simulations of 249 years using a global model with fully interactive ocean, chemistry, varying solar, and an internally generated QBO. This model provides all the forcings necessary to show any potential solar–QBO interaction. We therefore can look for the mean response of the atmosphere to the combined effects of solar cycle and QBO and investigate the physics leading to the response. We do not, however, find a significant correlation matching that seen in observations. Several possible reasons for the lack of a robust signal are discussed in this paper. One is that the observational record is relatively short and may be insufficient to separate out impacts of other forcing or atmospheric variability. Analyses over subsets of the model period strongly support the conclusion that this is a leading cause of the difference between the simulated and observed results.

There is also a possibility that WACCM4 is missing one or more key components of the physics. The discussion above mentions the reasons for concluding that the possible impact of a discrepancy in the simulated QBO is small. There may also be an underestimation of the response of the tropical stratosphere to solar UV changes although this should only affect the magnitude, not the sign, of the response; it therefore is also not a likely explanation for the model difference with the observational record. Another possibility, not discussed above, is that the atmospheric response is caused by some aspect of the solar variability that is not included in WACCM4. Gray et al. (2010) list the many solar forcing influences on the atmosphere, such as variability in energetic particle precipitation, which may impact ozone in the stratosphere and thereby alter the temperature gradient, stratospheric winds, and planetary waves (Randall et al., 2005). WACCM4 includes solar variability of particle impacts in the thermosphere but does not simulate the higher energy particles that sometimes penetrate into the middle or lower atmosphere. If these play a role in the dynamical response of the stratosphere to the solar cycle, their impact will not be seen in these simulations. There may also be a combination of factors acting together, as proposed by Meehl et al. (2009).

Acknowledgements. Part of this work was supported under NOAA Award NA09NES4400016. NCAR is sponsored by the National Science Foundation. Resources supporting this work were provided by the NASA High-End Computing (HEC) Program through the NASA Advanced Supercomputing (NAS) Division at Ames Research Center, and NASA LWS Strategic Capability grant NNX09AJ83G. The authors thank the two anonymous reviewers who provided constructive comments, which helped to greatly improve the manuscript. Wavelet software to produce the wavelet power spectrum was provided by C. Torrence and G. Compo, and is available at: http://paos.colorado.edu/research/wavelets/.

Edited by: W. Ward

References

Anstey, J. A. and Shepherd, T. G.: High-latitude influence of the quasi-biennial oscillation, Q. J. Roy. Meteor. Soc., 140, 1–21, doi:10.1002/qj.2132, 2014.

Austin, J., Tourpali, K., Rozanov, E., Akiyoshi, H., Bekki, S., Bodeker, G., Bruhl, C., Butchart, N., Chipperfield, M., Deushi, M., Fomichev, V. I., Giorgetta, M. A., Gray, L., Kodera, K., Lott, F., Manzini, E., Marsh, D., Matthes, K., Nagashima, T., Shibata, K., Stolarski, R. S., Struthers, H., and Tian, W.: Coupled chemistry climate model simulations of the solar cycle in ozone and temperature, J. Geophys. Res., 113, D11306, doi:10.1029/2007JD009391, 2008.

Balachandran, N. K. and Rind, D.: Modeling the Effects of UV Variability and the QBO on the Troposphere-Stratosphere System. Part I: The Middle Atmosphere, J. Climate, 8, 2058–2079, doi:10.1175/1520-0442(1995)008<2058:MTEOUV>2.0.CO;2, 1995.

Baldwin, M. P., Gray, L. J., Dunkerton, T. J., Hamilton. K., Haynes, P. H., Randel, W. J., Holton, J. R., Alexander, M. J., Hirota, I., Horinouchi, T., Jones, D. B. A., Kinnersley, J. S., Marquardt, C., Sato, K., and Takahashi, M.: The quasi-biennial oscillation, Rev. Geophys., 39, 179–229, doi:10.1029/1999RG000073, 2001.

Baliunas, S. and Jastrow, R.: Evidence for long-term brightness changes in solar-type stars, Nature, 348, 520–522, 1990.

Bard, E., Raisbeck, G., Yiou, F., and Jouzel, J.: Tellus B, 52, 985–992, doi:10.1034/j.1600-0889.2000.d01-7.x, 2000.

Camp, C. D. and Tung, K.: The Influence of the Solar Cycle and QBO on the Late-Winter Stratospheric Polar Vortex, J. Atmos. Sci., 64, 1267–1283, doi:10.1175/JAS3883.1, 2007.

Chiodo, G., Calvo, N., Marsh, D. R., and Garcia-Herrera, R.: The 11 year solar cycle signal in transient simulations from the Whole Atmosphere Community Model, J. Geophys. Res., 117, D06109, doi:10.1029/2011JD016393, 2012.

Chiodo, G., Marsh, D. R., Garcia-Herrera, R., Calvo, N., and García, J. A.: On the detection of the solar signal in the tropical stratosphere, Atmos. Chem. Phys. Discuss., 13, 30097–30142, doi:10.5194/acpd-13-30097-2013, 2013.

Ermolli, I., Matthes, K., Dudok de Wit, T., Krivova, N. A., Tourpali, K., Weber, M., Unruh, Y. C., Gray, L., Langematz, U., Pilewskie, P., Rozanov, E., Schmutz, W., Shapiro, A., Solanki, S. K., and Woods, T. N.: Recent variability of the solar spectral irradiance and its impact on climate modelling, Atmos. Chem. Phys., 13, 3945–3977, doi:10.5194/acp-13-3945-2013, 2013.

Fischer, P. and Tung, K. K.: A reexamination of the QBO period modulation by the solar cycle, J. Geophys. Res., 113, D07114, doi:10.1029/2007JD008983, 2008.

Garfinkel, C. I., Shaw, T. A., Hartmann, D. L., and Waugh, D. W.: Does the Holton-Tan Mechanism Explain How the Quasi-Biennial Oscillation Modulates the Arctic Polar Vortex?, J. Atmos. Sci., 69, 1713–1733, doi:10.1175/JAS-D-11-0209.1, 2012.

Giorgetta, M. A., Manzini, E., and Roeckner, E.: Forcing of the quasi-biennial oscillation from a broad spectrum of atmospheric waves, Geophys. Res. Lett., 29, 86-1–86-4,, doi:10.1029/2002GL014756, 2002.

Giorgetta, M. A., Manzini, E., Roeckner, E., Esch, M., and Bengtsson, L.: Climatology and Forcing of the Quasi-Biennial Oscillation in the MAECHAM5 Model, J. Climate, 19, 3882–3901, doi:10.1175/JCLI3830.1, 2006.

Gray, L. J., Crooks, S., Pascoe, C., Sparrow, S., and Palmer, M.: Solar and QBO Influences on the Timing of Stratospheric Sudden Warmings, J. Atmos. Sci., 61, 2777–2796, doi:10.1175/JAS-3297.1, 2004.

Gray, L. J., Crooks, S. A., Palmer, M. A., Pascoe, C. L., and Sparrow, S.: A possible transfer mechanism for the 11-year solar cycle to the lower stratosphere, Space Sci. Rev., 125, 357–370, doi:10.1007/s11214-006-9069-y, 2006.

Gray, L. J., Beer, J., Geller, M., Haigh, J. D., Lockwood, M., Matthes, K., Cubasch, U., Fleitmann, D., Harrison, G., Hood, L., Luterbacher, J., Meehl, G. A., Shindell, D., van Geel, B., and White, W: Solar influences on climate, Rev. Geophys., 48, RG4001, doi:10.1029/2009RG000282, 2010.

Holton, J. R. and Tan, H.: The Influence of the Equatorial Quasi-Biennial Oscillation on the Global Circulation at 50 mb, J. Atmos. Sci., 37, 2200–2208, doi:10.1175/1520-0469(1980)037<2200:TIOTEQ>2.0.CO;2, 1980.

Kalnay, E., Kanamitsu, M., Kistler, R., Collins, W., Deaven, D., Gandin, L., Iredell, M., Saha, S., White, G., Woollen, J., Zhu, Y., Chelliah, M., Ebisuzaki, W., Higgins, W., Janowiak, J., Mo, K. C., Ropelewski, C., Wang, J., Leetmaa, A., Reynolds, R., Jenne, R., and Joseph, D.: The NCEP/NCAR 40-Year Reanalysis Project, B. Am. Meteorol. Soc., 77, 437–470, 1996.

Kistler, R., Collins, W., Saha, S., White, G., Woollen, J., Kalnay, E., Chelliah, M., Ebisuzaki, W., Kanamitsu, M., Kousky, V., van den Dool, H., Jenne, R., and Fiorino, M.: The NCEP-NCAR 50-Year Reanalysis: Monthly Means CD-ROM and Documentation, B. Am. Meteorol. Soc., 82, 247–267, doi:10.1175/1520-0477(2001)082<0247:TNNYRM>2.3.CO;2, 2001.

Kodera, K.: The solar and equatorial QBO influences on the stratospheric circulation during early northern-hemisphere winter, Geophys. Res. Lett., 18, 1023–1026, doi:10.1029/90GL02298, 1991.

Kodera, K. and Kuroda, Y.: Dynamical response to the solar cycle, J. Geophys. Res., 107, 4749, doi:10.1029/2002JD002224, 2002.

Kopp, G. and Lean, J. L.: A new, lower value of irradiance: Evidence and climate significance, Geophys. Res. Lett., 38, L01706, doi:10.1029/2010GL045777, 2011.

Labitzke, K.: Sunspots, the QBO, and the stratospheric temperature in the north polar region, Geophys. Res. Lett., 14, 535–537, doi:10.1029/GL014i005p00535, 1987.

Labitzke, K.: On the solar cycle-QBO relationship: a summary, J. Atmos. Sol-Terr. Phy., 67, 45–54, doi:10.1016/j.jastp.2004.07.016, 2005.

Labitzke, K. and Kunze, M.: On the remarkable Arctic winter in 2008/2009, J. Geophys. Res., 114, D00I02, doi:10.1029/2009JD012273, 2009.

Labitzke, K., and van Loon, H.: Associations between the 11-year solar cycle, the QBO and the atmosphere. Part I: the troposphere and stratosphere in the northern hemisphere in winter, J. Atmos. Terr. Phys., 50, 197–206, doi:10.1016/0021-9169(88)90068-2, 1988.

Labitzke, K. and van Loon, H.: The QBO effect on the solar signal in the global stratosphere in the winter of the Northern Hemisphere, J. Atmos. Sol.-Terr. Phy., 62, 621–628, 2000.

Lean, J.: Evolution of the Sun's Spectral Irradiance Since the Maunder Minimum, Geophys. Res. Lett., 27, 2425–2428, doi:10.1029/2000GL000043, 2000.

Lean, J. L., Rottman, G. J., Kyle, H. L., Woods, T. N., Hickey, J. R., and Puga, L. C.: Detection and parameterization of variations in solar mid- and near-ultraviolet radiation (200–400 nm), J. Geophys. Res., 102, 29939–29956, doi:10.1029/97JD02092, 1997.

Lean, J., Rottman, G., Harder, J., and Kopp, G.: SORCE Contributions to New Understanding of Global Change and Solar Variability, Sol. Phys., 230, 27–53, doi:10.1007/s11207-005-1527-2, 2005.

Lee, H. and Smith, A. K.: Simulation of the combined effects of solar cycle, quasi-biennial oscillation, and volcanic forcing on stratospheric ozone changes in recent decades, J. Geophys. Res., 108, D24049, doi:10.1029/2001JD001503, 2003.

Lockwood, M. and Stamper, R.: Long term drift in the coronal source magnetic flux and the total solar irradiance, Geophys. Res. Lett., 26, 2461–2465, 1999.

Lu, H., Baldwin, M. P., Gray, L. J., and Jarvis, M. J.: Decadal-scale changes in the effect of the QBO on the northern stratospheric polar vortex, J. Geophys. Res., 113, D10114, doi:10.1029/2007JD009647, 2008.

Lu, H., Gray, L. J., Baldwin, M. P., and Jarvis, M. J.: Life cycle of the QBO-modulated 11-year solar cycle signals in the Northern Hemispheric winter, Q. J. Roy. Meteor. Soc., 135, 1030–1043, doi:10.1002/qj.419, 2009.

Marsh, D. R., Garcia, R. R., Kinnison, D. E., Boville, B. A., Sassi, F., Solomon, S. C., and Matthes, K.: Modeling the whole atmosphere response to solar cycle changes in radiative and geomagnetic forcing, J. Geophys. Res., 112, D23306, doi:10.1029/2006JD008306, 2007.

Marsh, D. R., Mills, M. J., Kinnison, D. E., Lamarque, J.-F., Calvo, N., and Polvani, L. M.: Climate Change from 1850–2005 Simulated in CESM1(WACCM), J. Climate, 26, 7372–7391, doi:10.1175/JCLI-D-12-00558.1, 2013.

Matthes, K., Langematz, U., Gray, L. J., Kodera, K., and Labitzke, K.: Improved 11-year solar signal in the Freie Universitat Berlin Climate Middle Atmosphere Model (FUB-CMAM), J. Geophys. Res., 109, D06101, doi:10.1029/2003JD004012, 2004.

Matthes, K., Marsh, D. R., Garcia, R. R., Kinnison, D. E., Sassi, F., and Walters, S.: Role of the QBO in modulating the influence of the 11 year solar cycle on the atmosphere using constant forcings, J. Geophys. Res., 115, D18110, doi:10.1029/2009JD013020, 2010.

Matthes, K., Kodera, K., Garcia, R. R., Kuroda, Y., Marsh, D. R., and Labitzke, K.: The importance of time-varying forcing for QBO modulation of the atmospheric 11 year solar cycle signal, J. Geophys. Res. Atmos., 118, 4435–4447, doi:10.1002/jgrd.50424, 2013.

McCormack, J. P.: The influence of the 11-year solar cycle on the quasi-biennial oscillation, Geophys. Res. Lett., 30, 2162, doi:10.1029/2003GL018314, 2003.

McCormack, J. P., Siskind, D. E., and Hood, L. L.: Solar-QBO interaction and its impact on stratospheric ozone in a zonally averaged photochemical transport model of the middle atmosphere, J. Geophys. Res., 112, D16109, doi:10.1029/2006JD008369, 2007.

Meehl, G. A., Arblaster, J. M., Matthes, K., Sassi, F., and van Loon, H: Amplifying the Pacific Climate System Response to a Small 11-Year Solar Cycle Forcing, Science, 325, 1114–1118, doi:10.1126/science.1172872, 2009.

Naoe, H. and Shibata, K.: Equatorial quasi-biennial oscillation influence on northern winter extratropical circulation, J. Geophys. Res., 115, D19102, doi:10.1029/2009JD012952, 2010.

Naujokat, B.: An Update of the Observed Quasi-Biennial Oscillation of the Stratospheric Winds over the Tropics, J. Atmos. Sci., 43, 1873–1877, doi:10.1175/1520-0469(1986)043<1873:AUOTOQ>2.0.CO;2, 1986.

Palmer, M. A. and Gray, L. J.: Modeling the atmospheric response to solar irradiance changes using a GCM with a realistic QBO, Geophys. Res. Lett., 32, L24701, doi:10.1029/2005GL023809, 2005.

Pascoe, C. L., Gray, L. J., Crooks, S. A., Juckes, M. N., and Baldwin, M. P.: The quasi-biennial oscillation: Analysis using ERA-40 data, J. Geophys. Res., 110, D08105, doi:10.1029/2004JD004941, 2005.

Randall, C. E., Harvey, V. L., Manney, G. L., Orsolini, Y., Codrescu, M., Sioris, C., Brohede, S., Haley, C. S., Gordley, L. L, Zawodny, J. M., and Russell III, J. M: Stratospheric effects of energetic particle precipitation in 2003–2004, Geophys. Res. Lett., 32, L05802, doi:10.1029/2004GL022003, 2005.

Rind, D. and Balachandran, N. K.: Modeling the Effects of UV Variability and the QBO on the Troposphere-Stratosphere System. Part II: The Troposphere, J. Climate, 8, 2080–2095, doi:10.1175/1520-0442(1995)008<2058:MTEOUV>2.0.CO;2, 1995.

Rottman, G.: The SORCE Mission, Sol. Phys., 230, 7-25, doi:10.1007/0-387-37625-9_2, 2005.

Rottman, G., Floyd, L., and Viereck, R.: Measurement of the Solar Ultraviolet Irradince, in: Solar Variability and its Effects on Climate. Geophysical Monograph 141, edited by: Pap, J. M., Fox, P., Fröhlich, C., Hudson, H. S., Kuhn, J., McCormack, J., North, G., Sprigg, W., and Wu, S. T., Vol. 141 of Washington DC American Geophysical Union Geophysical Monograph Series, 111–125, 2004.

Salby, M. and Callaghan, P.: Connection between the Solar Cycle and the QBO: The Missing Link*, J. Climate, 13, 2652–2662, doi:10.1175/1520-0442(1999)012<2652:CBTSCA>2.0.CO;2, 2000.

Salby, M. and Callaghan, P.: Evidence of the Solar Cycle in the General Circulation of the Stratosphere, J. Climate, 17, 34–46, doi:10.1175/1520-0442(2004)017<0034:EOTSCI>2.0.CO;2, 2004.

Salby, M. L. and Callaghan, P.: Relaionship of the quasi-biennial oscillation to the stratospheric signature of the solar cycle, J. Geophys. Res., 111, D06110, doi:10.1029/2005JD006012, 2006.

Salby, M. and Shea, D.: Correlations between solar activity and the atmosphere: an unphysical explanation, J. Geophys. Res., 96, 22579–22595, doi:10.1029/91JD02530, 1991.

Schmidt, H., Brasseur, G. P., and Giorgetta, M. A.: Solar cycle in a general circulation and chemistry model with internally generated quasi-biennial oscillation, J. Geophys. Res., 115, D00I14, doi:10.1029/2009JD012542, 2010.

SPARC CCMVal: SPARC CCMVal Report on the Evaluation of Chemistry-Climate Models, edited by: Eyring, V., Shepherd, T. G., and Waugh, D. W., SPARC Report No. 5, WCRP-135, WMO/TD-No. 1526, 2010.

Taylor, K. E., Stouffer, R. J., and Meehl, G. A.: An Overview of CMIP5 and the Experiment Design, B. Am. Meteorol. Soc., 93, 485–498, doi:10.1175/BAMS-D-11-00094.1, 2012.

Thompson, W. J., Baldwin, M. P., and Wallace, J. M.: Stratospheric Connection to Northern Hemisphere Wintertime Weather: Implications for Prediction, J. Climate, 15, 1421–1428, 2002.

Thuillier, G., Foujols, T., Bolseìe, D., Gillotay, D., Herseì, M., Peetermans, W., Decuyper, W., Mandel, H., Sperfeld, P., Pape, S., Taubert, D. R., and Hartmann, J.: SOLAR/SOLSPEC: Scientific Objectives, Instrument Performance and Its Absolute Calibration Using a Blackbody as Primary Standard Source, Sol. Phys., 257, 185–213, doi:10.1007/s11207-009-9361-6, 2009.

Tilmes, S., Garcia, R. R., Kinnison, D. E., Gettelman, A., and Rasch, P. J.: Impact of geoengineered aerosols on the troposphere and stratosphere, J. Geophys. Res., 114, D12305, doi:10.1029/2008JD011420, 2009.

Torrence, C. and Compo, G. P.: A Practical Guide to Wavelet Analysis, B. Am. Meteorol. Soc., 79, 61–78, doi:10.1175/1520-0477(1998)079<0061:APGTWA>2.0.CO;2, 1998.

Watson, P. A. G and Gray, L. J.: How Does the Quasi-Biennial Oscillation Affect the Stratospheric Polar Vortex, J. Atmos. Sci., 71, 391–409, doi:10.1175/JAS-D-13-096.1, 2014.

Xue, X.-H., Liu, H.-L., and Dou, X.-K.: Parameterization of the inertial gravity waves and generation of the quasi-biennial oscillation, J. Geophys. Res., 117, D06103, doi:10.1029/2011JD016778, 2012.